Neuron 49, 341–348, February 2, 2006 ©2006 Elsevier Inc. DOI 10.1016/j.neuron.2005.12.027

The Disease Progression of *Mecp2* Mutant Mice Is Affected by the Level of BDNF Expression

Report

Qiang Chang,[1] Gargi Khare,[2] Vardhan Dani,[3] Sacha Nelson,[3] and Rudolf Jaenisch[1,2,*]
[1] Whitehead Institute for Biomedical Research
Cambridge, Massachusetts 02142
[2] Department of Biology
Massachusetts Institute of Technology
Cambridge, Massachusetts 02142
[3] Department of Biology and
Volen Center for Complex Systems
Brandeis University
Waltham, Massachusetts 02454

Summary

Mutations in the *MECP2* gene cause Rett syndrome (RTT). *Bdnf* is a MeCP2 target gene; however, its role in RTT pathogenesis is unknown. We examined *Bdnf* conditional mutant mice for RTT-relevant pathologies and observed that loss of BDNF caused smaller brain size, smaller CA2 neurons, smaller glomerulus size, and a characteristic hindlimb-clasping phenotype. BDNF protein level was reduced in *Mecp2* mutant mice, and deletion of *Bdnf* in *Mecp2* mutants caused an earlier onset of RTT-like symptoms. To assess whether this interaction was functional and potentially therapeutically relevant, we increased BDNF expression in the *Mecp2* mutant brain with a conditional *Bdnf* transgene. BDNF overexpression extended the lifespan, rescued a locomotor defect, and reversed an electrophysiological deficit observed in *Mecp2* mutants. Our results provide in vivo evidence for a functional interaction between *Mecp2* and *Bdnf* and demonstrate the physiological significance of altered BDNF expression/signaling in RTT disease progression.

Introduction

Rett syndrome (RTT), first described by Andreas Rett in 1966, is a neurological disorder that predominantly affects girls (Hagberg, 1985; Hagberg and Hagberg, 1997). The disease occurs in children of all races and has an estimated prevalence of 1 in 10,000–15,000 girls. The first sign of illness is the deceleration of head growth that begins between 2 and 4 months of age. Patients show rapid developmental regression between the ages of 1 to 3 years. Predominant features include social withdrawal, loss of previously acquired skills, including purposeful hand use and expressive language, and gait ataxia. At this stage, many patients also develop stereotypic movement of the hands and autonomic dysfunctions such as respiratory distress. With extensive care, patients may survive into adulthood, yet they are severely mentally retarded.

Mutations in the X-linked *MECP2* gene (methyl-CpG binding protein 2) account for close to 80% of RTT cases (Amir et al., 1999; Van den Veyver and Zoghbi, 2000; Wan et al., 1999; Xiang et al., 2000). To study the RTT disease mechanism, we and others established mouse models by engineering *Mecp2* gene deletions (Chen et al., 2001; Guy et al., 2001; Shahbazian et al., 2002). Mutant males develop normally until 5 weeks of age, when the first manifestations resembling RTT-like symptoms are observed, including reduced brain weight, decreased CA2 neuron size, hindlimb clasping, and impaired locomotor function (Chen et al., 2001; Guy et al., 2001).

MeCP2 was initially identified as a protein that specifically binds to methylated DNA in vitro and represses transcription from methylated promoters both in vitro and in vivo (Lewis et al., 1992; Nan et al., 1997). MeCP2 associates with a core repressor complex containing the transcriptional repressor mSin3A and histone deacetylases (Jones et al., 1998), suggesting that MeCP2 may function as a molecular linker between DNA methylation, chromatin remodeling, and subsequent gene silencing (Bird and Wolffe, 1999). Yet, relatively few expression changes have been identified in *Mecp2* mutants that might explain the underlying molecular basis for RTT disease progression (Chen et al., 2003; Horike et al., 2005; Nuber et al., 2005; Tudor et al., 2002). And the functional consequences of these expression changes have not been studied in vivo. In addition, MeCP2 was recently implicated in regulating RNA splicing (Young et al., 2005).

One MeCP2 target is a neuronal activity-dependent gene, *Bdnf*, which encodes a neurotrophic factor essential for neuronal survival (Bonni et al., 1999), differentiation (Ghosh et al., 1994), and synaptic plasticity (Poo, 2001). In cultured neonatal cortical neurons, basal *Bdnf* transcription is repressed by MeCP2 in the absence of neuronal activity, but activity-dependent upregulation of *Bdnf* is unaffected by *Mecp2* deletion (Chen et al., 2003). Based on these results, one would predict that, when all the neurons are silent, the *Mecp2* mutant brain should express more BDNF than the wild-type brain does at the basal level; yet when all the neurons are active, the *Mecp2* mutant brain should express the same amount of BDNF as the wild-type brain does at the highly induced level. However, these predictions are made under the assumption that the level of neuronal activity is the same in both the wild-type and *Mecp2* mutant brain. We recently reported reduced cortical activity in the *Mecp2* mutant brain (Dani et al., 2005), which may lead to lack of activation of *Bdnf* upregulation in the *Mecp2* mutant brain. Indeed, we show here that BDNF protein level in the whole-brain lysate in *Mecp2* mutant mice is decreased to about 70% of the wild-type level. We also observed similar phenotypes between the conditional *Bdnf* mutant mice and the *Mecp2* mutant mice, suggesting that the moderate decrease in BDNF protein level may mediate some defects in the *Mecp2* mutant mice. To further investigate the in vivo role of BDNF in RTT, we manipulated BDNF expression in the postnatal brains of *Mecp2*-deficient mice. We discovered that deleting *Bdnf* from the *Mecp2* mutant brain resulted in an earlier onset/accelerated disease progression, whereas overexpressing BDNF in the *Mecp2* mutant brain led to later onset/slower disease progression. Our findings provide

*Correspondence: jaenisch@wi.mit.edu

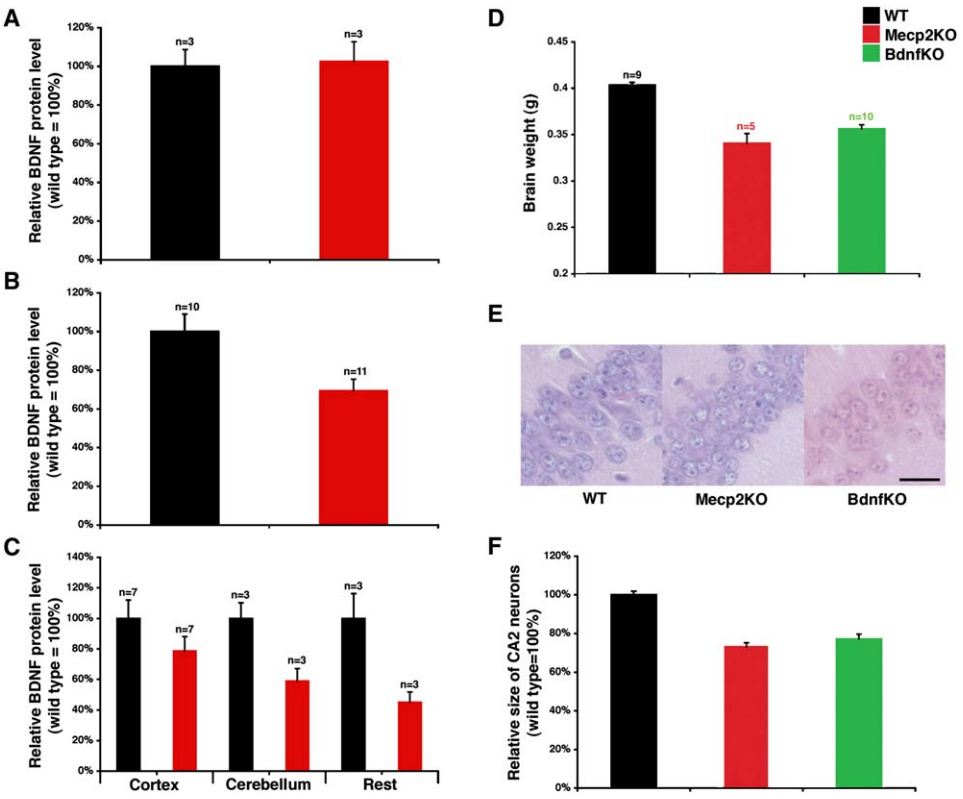

Figure 1. Lower Level of BDNF Protein in *Mecp2* Mutant Brain and Phenotypic Similarities between *Bdnf* and *Mecp2* Deficiencies

(A–C) An ELISA assay was used to quantify the amount of total BDNF protein in either the whole brain or subregions of the brain from *Mecp2* mutant mice (Mecp2KO) and wild-type littermates (WT). N indicates the number of samples assayed in each genotype. Wild-type level was set at 100%. Mecp2KO level was normalized against WT. All p values are from Student's t tests. (A) At 2 weeks of age, no difference in BDNF protein level was detectable between the Mecp2KO and the WT brains (103% versus 100%, p = 0.81). (B) At 6–8 weeks of age, Mecp2KO brains have less BDNF protein than the WT brains (69% versus 100%, p = 0.01). (C) At 6–8 weeks of age, Mecp2KO mice express less BDNF protein in the cortex (79% versus 100%, p = 0.005), the cerebellum (59% versus 100%, p = 0.009), and the rest of the brain (45% versus 100%, p = 0.01). (D) Brains from nine wild-type (WT), five *Mecp2* mutant (Mecp2KO), and ten *Bdnf* conditional knockout (BdnfKO) mice were freshly isolated and weighed. Student's t test was performed. The p values were: Mecp2KO versus WT, p = 0.0028; BdnfKO versus WT, p = 1.3E-07; and BdnfKO versus Mecp2KO, p = 0.22. (E) Representative pictures of the hippocampal CA2 region of each indicated genotype. Neuronal cell bodies were stained with Hematoxlin (purple). The sections were counterstained with Eosin (pink). Scale bar = 50 μm. (F) At least 150 clearly stained neurons (i.e., most of the ones shown in [E]) from three mice in each genotype were measured, using the OpenLab software. The area occupied by each neuronal soma was measured by arbitrary units. Cell size of each genotype was normalized against the wild-type. A Student's t test was performed to compare Mecp2KO with WT (p = 7.6E-14), BdnfKO with WT (p = 1.4E-10), and BdnfKO with Mecp2KO (p = 0.81). Data are presented as mean ± SEM in all the bar graphs in this figure.

in vivo evidence of a functional interaction between *Mecp2* and *Bdnf*. Furthermore, our results indicate that manipulating the BDNF level or the BDNF signaling pathways may present therapeutic opportunities for RTT patients.

Results

Mecp2 Mutant Mice Express Decreased Levels of BDNF Protein

We used an ELISA assay to measure the level of BDNF protein in whole-brain protein extracts prepared from wild-type and *Mecp2* mutants. At the presymptomatic stage (2 weeks of age), no difference was detectable between mutant and wild-type mice (Figure 1A). However, at an age when mice become symptomatic (6–8 weeks of age), we found that the BDNF protein level in *Mecp2* mutant brains was 69% of the wild-type level (p = 0.01, Figure 1B). To find out whether BDNF protein level is decreased throughout the brain or in specific subregions of the brain, we separated the brain into cortex, cerebellum, and the rest of the brain and again performed the ELISA assay. Because BDNF protein levels were decreased in mice displaying the typical mutant phenotype but not in mice at the presymptomatic stage, we examined brain subregions of symptomatic animals. At 7–8 weeks of age, we detected reduced levels of BDNF in all three subdivisions of the brain (Figure 1C, 79% of the wild-type in the Mecp2KO cortex, p = 0.005; 59% of the wild-type in the Mecp2KO cerebellum, p = 0.009; and 45% of the wild-type in the rest of the Mecp2KO brain, p = 0.01, respectively).

Phenotypic Similarities between the Conditional *Bdnf* Knockout Mice and the *Mecp2* Mutant Mice

To assess whether the decreased BDNF protein level may be involved in the neurological defects seen in *Mecp2* mutant mice, we investigated whether *Bdnf* and

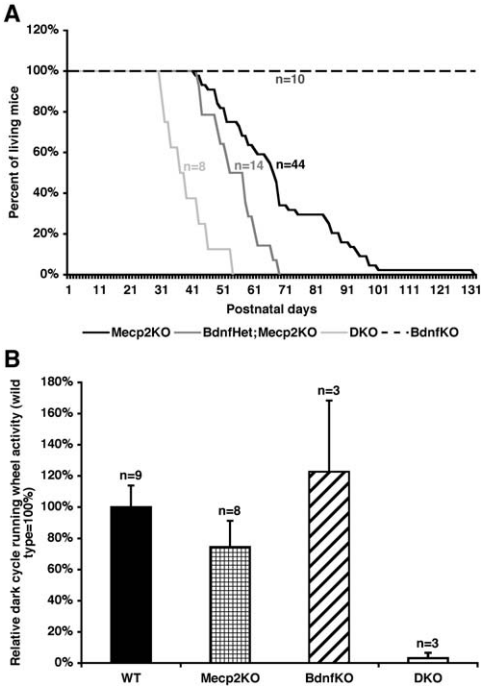

Figure 2. *Bdnf* Deletion in the *Mecp2* Mutant Brain Resulted in an Earlier Onset of RTT

(A) Survival curve of each specified genotype was generated by plotting the percentage of live mice (y axis) in that genotype against the postnatal days (x axis). N is the total number of mice included in each genotype. The black line is the survival curve of the *Mecp2* mutant (Mecp2KO) mice. The dashed line is the survival curve of the *Mecp2*$^{+/y}$;cre93;*Bdnf*$^{2lox/2lox}$ (BdnfKO) mice. The medium gray line is the survival curve of the *Mecp2*$^{-/y}$;cre93;*Bdnf*$^{2lox/+}$ (BDNFhet; Mecp2KO) mice. The light gray line is the survival curve of the *Mecp2*$^{-/y}$;cre93;*Bdnf*$^{2lox/2lox}$ (DKO) mice. A log rank test (Harrington and Fleming, 1982) was performed to assess the statistical significance in the difference among the survival curves: BDNFhet; Mecp2KO versus Mecp2KO mice (p = 0.0096), DKO versus BDNFhet;Mecp2KO (p = 0.00031), and DKO versus Mecp2KO (p = 1.3E-07). Because the wild-type mice (WT) did not die during the time window studied here, their survival curve was not plotted in the graph. (B) A running-wheel assay was performed to assess the *Bdnf* deletion on the locomotor function of the *Mecp2* mutant mice at 4 weeks of age. Total wheel-running activity of the wild-type was set as 100%. The activity value in other genotypes was normalized against the wild-type value to calculate the relative activity. N above each bar indicates the number of mice included for that genotype. All p values were from Student's t tests: Mecp2KO versus WT (p = 0.18), BdnfKO versus WT (p = 0.77), DKO versus WT (p = 0.0002). Data are presented as mean ± SEM in all the bar graphs in this figure.

Mecp2 mutant mice display phenotypic similarities. Because germline *Bdnf* knockout mice die shortly after birth (Ernfors et al., 1994), we examined conditional *Bdnf* knockout mice that were generated previously by cre-mediated (cre93 transgene) deletion of a floxed *Bdnf* allele in postmitotic neurons throughout the forebrain, part of the midbrain, and hindbrain structures (Fan et al., 2001; Rios et al., 2001). Although *Bdnf* and *Mecp2* mutants display significant phenotypic differences, we detected some anatomical and functional similarities between the respective mutants. As found in *Mecp2* mutant mice, the average brain weight of *Bdnf* mutant mice was smaller than in wild-type animals (Figure 1D). A smaller brain weight is one of the pathological characteristics of RTT patients(Hagberg and Hagberg, 1997). Furthermore, the size of CA2 neurons, as well as the size of olfactory glomeruli (a specialized synapse in the olfactory bulb), was reduced in both the *Bdnf* and the *Mecp2* mutant mice as compared to their respective wild-type littermates (Figures 1E and 1F and Figure S1 in the Supplemental Data available with this article online). Both the decrease of neuronal size (Chen et al., 2001) and of the olfactory glomeruli size have been previously described in *Mecp2* mutants (Matarazzo et al., 2004). Finally, we observed a hindlimb-clasping phenotype in *Bdnf* mutant mice (Figure S2), which has been reported in *Mecp2* mutants (Guy et al., 2001; Shahbazian et al., 2002) and is thought to mimic the stereotypic hand-wringing behavior in RTT patients. The phenotypic similarities between conditional *Bdnf* and *Mecp2* mutants are consistent with the possibility that BDNF may mediate part of the late RTT pathologies (such as the small brain/neuron/synapse defects). Although our data suggest that BDNF and MeCP2 may regulate similar processes in the brain, they do not distinguish whether the two genes function through parallel or linear pathways. Based on these observations, we hypothesized that changes in BDNF expression level may modulate disease progression in *Mecp2* mutant mice. We therefore tested whether deletion or overexpression of BDNF in the *Mecp2* mutant brain would exacerbate or alleviate, respectively, the RTT-like symptoms.

Deletion of *Bdnf* from the Postnatal *Mecp2* Mutant Brain Results in an Earlier Onset of RTT

To study how *Bdnf* deletion may affect disease progression in the *Mecp2* mutant mice, we crossed male *Mecp2*$^{+/y}$;cre93;*Bdnf*$^{2lox/+}$ mice with female *Mecp2*$^{+/-}$; *Bdnf*$^{2lox/+}$ mice to generate *Mecp2*$^{-/y}$;cre93;*Bdnf*$^{2lox/2lox}$ mice (DKO). When aged, the DKO mice showed a significantly shorter lifespan (light gray line, Figure 2A) than the *Mecp2* single-mutant mice (Mecp2KO) (black line, Figure 2A). Survival of the *Mecp2* mutants was affected by *Bdnf* dosage, because *Mecp2*$^{-/y}$;cre93;*Bdnf*$^{2lox/+}$ mice (BdnfHet;Mecp2KO, medium gray line) had a shorter lifespan than the Mecp2KO mice but survived longer than the DKO mice (Figure 2A). Because both the cre93;*Bdnf*$^{2lox/2lox}$ (BdnfKO, dashed line, Figure 2A) and the cre93;*Bdnf*$^{2lox/+}$ (BdnfHet) mice have normal lifespans (Rios et al., 2001), the effect of BDNF level on the survival of Mecp2KO mice may reflect a functional interaction of the two genes.

Mecp2 mutant mice become lethargic and display decreased locomotor activity beginning at 6 weeks of age (Chen et al., 2001). To test whether *Bdnf* deletion in the brain of *Mecp2* mutants may exacerbate locomotor dysfunction, we performed a dark-cycle locomotor activity assay (running-wheel assay). As shown in Figure 2B, the DKO mice showed a dramatically reduced level of running-wheel activity at 4 weeks of age, while neither the *Mecp2* single mutants nor the *Bdnf* single mutants performed significantly differently from the wild-type mice at this age (Figure 2B). Thus, postnatal Bdnf deletion in the brain of *Mecp2* mutants resulted in an earlier onset of locomotor dysfunction and earlier lethality than was seen in *Mecp2* single mutants.

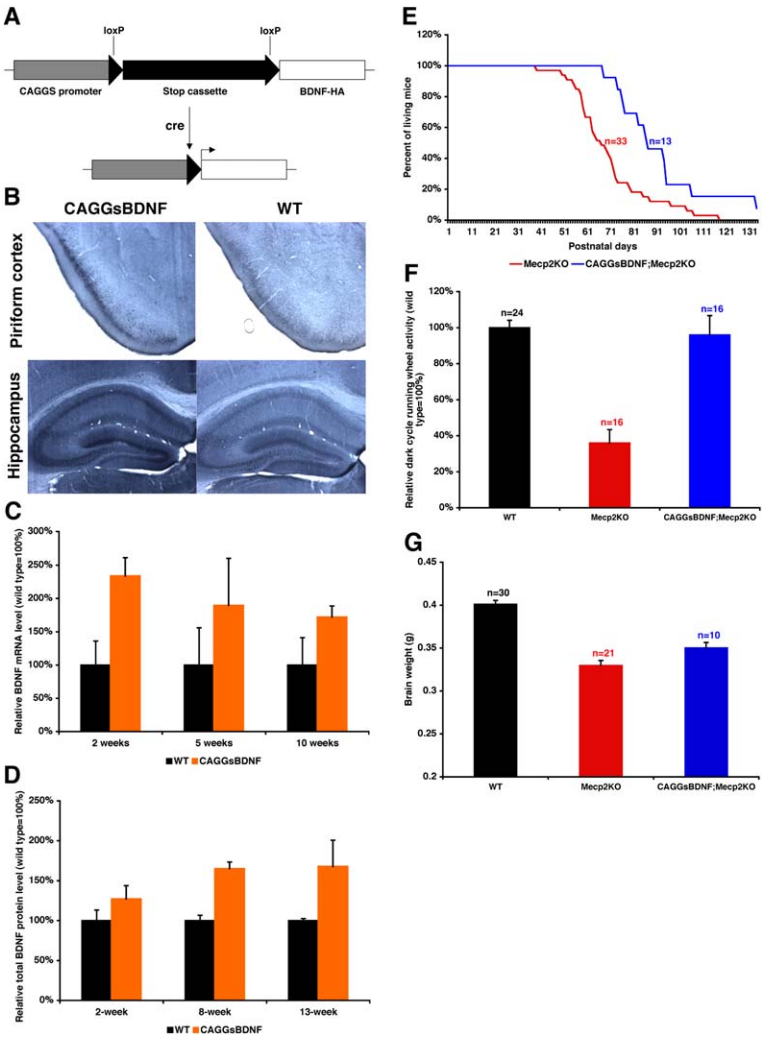

Figure 3. BDNF Overexpression in the *Mecp2* Mutant Brain Delayed the Onset of RTT

(A) Schematic representation of the conditional BDNF-overexpression allele at the collagen 1a1 locus before and after cre-mediated removal of the STOP cassette. (B) Representative pictures of the piriform cortex and the hippocampus stained with a BDNF-specific antibody. Note the signals in the pyramidal neurons in the piriform cortex and throughout the hippocampus were much stronger in the BDNF-overexpression mice (CAGGsBDNF, left) than the controls (WT, right). (C) A quantitative PCR assay was performed to assess the level of BDNF RNA in the cortex of BDNF-overexpression mice (CAGGsBDNF) as compared to the wild-type control. Three mice from each genotype were examined at each time point. (D) An ELISA assay was performed to assess the level of BDNF protein in the cortex of BDNF-overexpression mice (CAGGsBDNF) as compared to the wild-type control. Three mice from each genotype were examined at each time point. (E) Survival curve of each specified genotype was generated by plotting the percentage of live mice (y axis) in that genotype against the postnatal days (x axis). N is the total number of mice included in each genotype. The red line is the survival curve of the *Mecp2* mutant (Mecp2KO) mice. The blue line is the survival curve of the Mecp2 mutant mice that also overexpress BDNF (CAGGsBDNF;Mecp2KO). A log rank test was performed to assess the statistical significance in the difference between the survival curves of the CAGGsBDNF;Mecp2KO mice and the Mecp2KO mice ($p = 0.003$). Because the wild-type mice (WT) did not die during the time window studied here, their survival curve was not plotted in the graph. (F) A running-wheel assay was performed to assess the BDNF overexpression on the locomotor function of the *Mecp2* mutant mice at 6 weeks of age. Total wheel-running activity of the wild-type was set as 100%. The activity value in other genotypes was normalized against the wild-type value to calculate the relative activity. N above each bar indicates the number of mice included for that genotype. All p values were from Student's t tests: Mecp2KO versus WT ($p = 3E-07$), CAGGsBDNF;Mecp2KO versus WT ($p = 0.71$), and CAGGsBDNF;Mecp2KO versus Mecp2KO ($p = 9E-05$). (G) Brain weight was used as a crude measure to assess the effect of BDNF overexpression on the size of *Mecp2* mutant brain. The value bars represent the average brain weight of each indicated genotype. The error bars represent SEM. N above each bar indicates the number of mice included for that genotype. All p values were from Student's t tests. The average brain weight from the CAGGsBDNF;Mecp2KO mice was modestly higher than that from the Mecp2KO mice (0.350 g versus 0.329 g, $p = 0.026$). However, the size of the CAGGsBDNF;Mecp2KO brain was still significantly smaller than their wild-type littermates (0.350 g versus 0.401 g, $p = 3.2E-06$). Data are presented as mean ± SEM in all the bar graphs in this figure.

Generation of a Conditional BDNF-Overexpressing Allele

We next tested whether BDNF overexpression may delay the onset or alleviate the RTT-like symptoms in *Mecp2* mutant mice. We engineered a conditional *Bdnf* overexpression transgene using the human BDNF cDNA ($BDNF^{stop}$) under regulation by the synthetic CAGGS promoter/enhancer/intron followed by a loxP-STOP-loxP cassette. The transgene was targeted downstream of the collagen 1a1 locus by frt/Flpase-mediated site-specific integration (Beard et al., 2005; Hochedlinger et al., 2005) in V6.5 ES cells, which were injected into blastocysts to create the conditional $BDNF^{stop}$ mice. In the presence of cre recombinase, the STOP cassette is removed, resulting in activation of the BDNF transgene (Figure 3A). We crossed the $BDNF^{stop}$ mice with the cre93 mice to generate the $BDNF^{stop}$;cre93 mice (CAGGs-BDNF), and we examined *Bdnf* RNA and protein levels at different ages. When compared to control mice, *Bdnf* RNA levels were increased between 1.7- and 2.4-fold at 2, 5, and 10 weeks of age (Figure 3C). Similarly, ELISA detected correspondingly increased levels of BDNF protein (Figure 3D). To investigate the spatial pattern of BDNF transgene expression, we performed immunohistochemistry on brain sections using a BDNF-specific antibody. When compared with control sections, ectopic BDNF-transgene expression was readily detectable in the pyramidal neurons in the cortex and hippocampus of the CAGGs-BDNF mice (Figure 3B), as well as in other brain structures where the cre transgene was expressed (data not shown), reflecting the activity of the cre93 transgene (Fan et al., 2001). Our results showed that cre93-mediated activation of the $BDNF^{stop}$ transgene resulted in an ~2-fold increase of BDNF

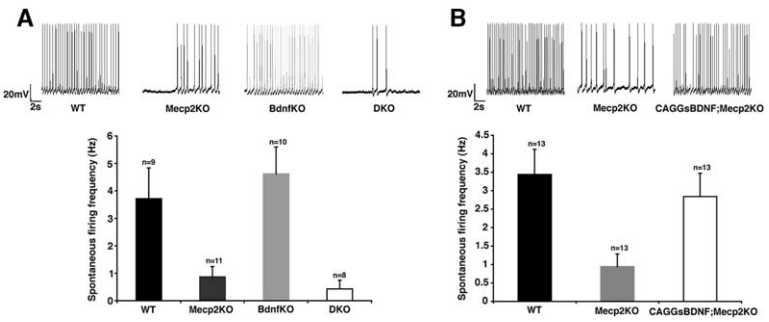

Figure 4. Effects of BDNF Deletion and Overexpression on Cortical Physiology of the *Mecp2* Mutant Mice

Whole-cell patch-clamp recordings were performed to assess the effect of *Bdnf* deletion and overexpression on spontaneous cortical activity in the *Mecp2* mutant mice. Spontaneous action potential spikes were recorded from layer 5 pyramidal neurons of the somatosensory cortex from each of the indicated genotypes at postnatal day 30. (Top) Representative traces from each indicated genotype. (Bottom) Quantification of all the recorded neurons. N above each bar indicates the number of neurons included for that genotype. All p values were from Student's t tests. p values in (A): Mecp2KO versus WT (p = 0.038), BdnfKO versus WT (p = 0.20), DKO versus WT (p = 0.019), and DKO versus Mecp2KO (p = 0.38). p values in (B): Mecp2KO versus WT (p = 0.004), CAGGsBDNF;Mecp2KO versus WT (p = 0.52), and CAGGsBDNF;Mecp2KO versus MT (p = 0.015). Data are presented as mean ± SEM in all the bar graphs in this figure.

expression. No obvious pathological defects were observed in the CAGGs-BDNF mice (data not shown).

Overexpressing BDNF in the *Mecp2* Mutant Brain Delayed the Onset of RTT

To test whether ectopic BDNF overexpression in *Mecp2* mutants influenced RTT-like symptoms, we crossed $BDNF^{stop}$ males with $Mecp2^{+/-}$;cre93 females to generate $Mecp2^{-/y}$;cre93;$BDNF^{stop}$ mice (CAGGsBDNF;Mecp2KO). In contrast to the reduced lifespan of DKO mice (compare Figure 2A), overexpression of BDNF resulted in a significantly increased lifespan (Figure 3E). Consistent with improved viability of the CAGGsBDNF;Mecp2KO mice, we observed functional improvement in the running-wheel assay described above. At 6 weeks of age, when the *Mecp2* mutant mice already show obvious symptoms, such as hindlimb clasping and reduced locomotor activity (Figure 3F), overexpression of BDNF resulted in a significant gain in locomotor function (Figure 3F).

One of the defects that are commonly observed in both human RTT patients and *Mecp2* mutant mice is reduced brain size (Chen et al., 2001; Hagberg, 1985; Hagberg and Hagberg, 1997) (Figure 1D). Although the functional consequence of such a size reduction remains unclear, our results indicate that both BDNF and MeCP2 can affect the brain/neuron size. Therefore, we were interested to know whether BDNF overexpression in the *Mecp2* mutant brain would partially rescue this defect. We observed a modest increase in brain weight in the CAGGsBDNF;Mecp2KO mice, compared to the Mecp2KO mice (Figure 3G, 0.35 g versus 0.329 g, p = 0.026).

Together, the common phenotypes seen in *Bdnf* and *Mecp2* mutants (Figures 1D–1F and Figures S1 and S2), the accelerated development of symptoms in mice with combined *Mecp2* and *Bdnf* deficiency (Figure 2), and the partial rescue of symptoms in *Mecp2* mutant mice that overexpress BDNF (Figure 3) demonstrate a functional interaction between these two genes.

Effects of BDNF Deletion and Overexpression on Cortical Physiology of the *Mecp2* Mutant Mice

To define the mechanistic basis to the interaction between *Bdnf* and *Mecp2*, we tested whether *Bdnf* deletion or BDNF overexpression affected electrophysiological properties in *Mecp2* mutant neurons. We performed whole-cell current-clamp recordings in layer 5 pyramidal neurons of the somatosensory cortex in mice of the respective genotypes based on our recent demonstration that acute slice preparations from *Mecp2* mutant mice displayed a reduced spontaneous activity as compared to the wild-type littermate controls (Dani et al., 2005). This defect was detectable in animals as young as 2 weeks of age and was most prominent in 5-week-old mutant mice. We investigated whether the deletion of *Bdnf* in *Mecp2* mutant neurons would further reduce the spontaneous firing rate. At postnatal day 30, consistent with our previous result, we found that the firing rate of layer 5 pyramidal neurons of the somatosensory cortex from the Mecp2KO slices was reduced as compared to wt controls (0.85 Hz versus 3.72 Hz, p = 0.0038, Figure 4A), while the firing rate in the BdnfKO slices was indistinguishable from the wt controls (4.62 Hz versus 3.72 Hz, p = 0.20). The averge firing rate of the DKO neurons was slightly lower than that of the Mecp2KO neurons (0.43 Hz versus 0.85 Hz, Figure 4A), though this was not statistically significant (p = 0.44). In contrast, we found a significantly increased firing rate in pyramidal neurons from *Mecp2* mutant mice that expressed ectopic BDNF when compared to the *Mecp2* single mutants (2.84 Hz versus 0.94 Hz, p = 0.015, Figure 4B). These results demonstrate that electrophysiological activity in *Mecp2* mutant neurons correlates with BDNF levels, which in turn are associated with locomotor function and viability, further substantiating the functional interaction between *Bdnf* and *Mecp2*.

Discussion

In neurons, BDNF expression is tightly regulated by neuronal activity. At increased activity levels, the mechanism of activity-dependent *Bdnf* transcription involves calcium influx through voltage-gated calcium channel (Ghosh et al., 1994), activation of Cam kinase IV (Shieh and Ghosh, 1999), and phosphorylation of CREB (Tao et al., 1998). Previously, we reported no difference in *Bdnf* RNA level (~100-fold of basal level) between *Mecp2*-deficient and wild-type neurons treated with KCl, which suggests that MeCP2 is not directly involved in the upregulation of *Bdnf* by increased activity (Chen et al., 2003). Yet, when treated with tetrodotoxin (TTX), which blocks activity, a 2-fold increase of the *Bdnf* RNA level was detected in *Mecp2*-deficient as compared to wild-type neurons. This suggests that MeCP2 may

function in the silencing of *Bdnf* basal transcription in activity-suppressed neurons (Chen et al., 2003). Our present results found a lower level of BDNF protein in mutant brains, an observation which is in apparent conflict with the previous results (Chen et al., 2003). To resolve this conflict, it is important to emphasize the differences in the previous and the present experimental design. Our previous experiments were performed in vitro and compared *Bdnf* RNA levels in homogeneous WT and Mecp2KO neuronal cultures where neuronal activity was artificially kept at an increased or suppressed level through KCl or TTX treatment, respectively. In contrast, the present study compared BDNF protein levels in wt (normal neuronal activity) and Mecp2KO (reduced neuronal activity) brains that are at different activity states. Given that BDNF expression depends on neuronal activity, we favor the hypothesis that *Mecp2* deficiency reduces neuronal activity, thereby indirectly causing a decreased BDNF protein level. Consistent with this possibility, we found progressively reduced neuronal activity in layer 5 pyramidal neurons in the somatosensory cortex of *Mecp2* mutant mice (Dani et al., 2005). This chronic reduced activity in a major class of BDNF-producing neurons in the *Mecp2* mutant brain is detectable at 2 weeks and may subsequently result in less activation of BDNF expression than the wild-type level. While our results demonstrate that the level of BDNF protein decreased in the *Mecp2* mutants, the molecular mechanism is not clear. Previous results, based upon neural cultures, have demonstrated that the basal transcription rate of *Bdnf* promoter III is regulated by MeCP2. It will be interesting to investigate whether the other *Bdnf* promoters are also affected in the *Mecp2* mutant brains.

BDNF is a well-known neurotrophic factor. The decreased level of BDNF protein in the *Mecp2* mutant brain may contribute to the small brain/neuron/synapse defect, a typical atrophic response caused by *Bdnf* deficiency. The phenotypic similarities between the *Mecp2* deficiency and the *Bdnf* deficiency are consistent with such a possibility. More importantly, the opposing effects of *Bdnf* deletion and overexpression on the survival, locomotor function, and cortical physiology of the *Mecp2* mutant mice are consistent with a functional interaction between BDNF and MeCP2 in RTT pathogenesis. Although our data do not distinguish whether MeCP2 and BDNF signal through parallel or linear pathways, they suggest that BDNF and MeCP2 may regulate the same biological process. It will be important to define what downstream targets of BDNF overlap with the affected targets in the *Mecp2* mutant mice.

Several aspects of the *Mecp2* mutant phenotype were ameliorated by postnatal ectopic expression of BDNF. For example, BDNF overexpression markedly improved the locomotor function of the *Mecp2* mutant mice in the dark-cycle running-wheel assay. It is possible that the improved motor function allows mutant mice more efficient access to food and water, which may, at least in part, explain the significant extension of lifespan. Furthermore, BDNF overexpression rescued an electrophysiological deficit in the *Mecp2* mutant cortex, resulting in an increased spontaneous firing of layer 5 pyramidal neurons. This result is consistent with many previous reports that studied the effect of BDNF on synaptic transmission (Schuman, 1999). It is possible that the overexpression of BDNF in *Mecp2* mutant brains also increased neuronal activity in other parts of the brain, such as the motor cortex, which contributed to the enhanced locomotor function.

Abnormal BDNF expression has been linked to many human diseases, such as Huntington's disease (Canals et al., 2004), schizophrenia, and depression (Angelucci et al., 2005). Our finding links *Bdnf* and *Mecp2* in vivo and suggests that RTT may be another human disease that is partially mediated through BDNF. Moreover, overexpression of such a pleotrophic factor in the brain has been shown to ameliorate symptoms in a mouse model of Huntington's disease (Cepeda et al., 2004; Kells et al., 2004). Similarly, our results suggest therapeutic opportunities through manipulation of BDNF expression. Although *Bdnf* is only one of many genes regulated by MeCP2, it is the first one shown to modulate disease progression of *Mecp2* mutant mice. Future studies will be aimed at understanding the molecular basis that underlies its effect on the course of RTT disease.

Experimental Procedures

Mice Mating and Genotyping

Many of the mouse alleles used in this study have been reported previously. These include the conditional *Bdnf* knockout allele (Rios et al., 2001), the cre93 transgene (Fan et al., 2001), and the *Mecp2* germline mutant allele (Chen et al., 2001). Genotyping of these alleles was performed as described in these papers. A PCR assay was developed to genotype the conditional BDNF overexpression allele. The primers are 5′-CCCTCCATGTGTGACCAAGG-3′ (col/frt-B); 5′-GCACAGCATTGCGGACATGC-3′ (col/frtA1); and 5′-GCAGAAGCG CGGCCGTCTGG-3′ (col/frtC1). A 551 bp band indicates a $BDNF^{stop}$ flip-in allele. A 300 bp band indicates a wild-type allele. Male $Bdnf^{2lox/+}$ mice were mated with female $Bdnf^{2lox/+}$;cre93 mice to generate $Bdnf^{2lox/2lox}$;cre93 mice (conditional *Bdnf* knockout mice). Male $Mecp2^{+/y}$;cre93;$Bdnf^{2lox/+}$ mice were mated with female $Mecp2^{+/-}$; $Bdnf^{2lox/+}$ mice to generate $Mecp2^{-/y}$;cre93;$Bdnf^{2lox/2lox}$ mice (DKO). Male $BDNF^{stop}$ mice were mated with female cre93 mice to generate $BDNF^{stop}$;cre93 mice (CAGGsBDNF mice). Male $BDNF^{stop}$ mice were mated with female $Mecp2^{+/-}$;cre93 mice to generate $Mecp2^{-/y}$;cre93;$BDNF^{stop}$ mice (CAGGsBDNF;Mecp2KO).

Generation of Conditional BDNF-Overexpressing Mice

An MluI/NotI fragment containing human BDNF cDNA with an HA tag was cut out from pAdCIG (a gift from Dr. Rita Balice-Gordon), blunt-ended, and ligated with an EcoRI cut/blunt-ended pCAGGSTurbo-cre vector to generate pCAGGS-BDNF-HA. A SpeI/SfiI fragment containing the CAGGS promoter, the BDNF cDNA, the HA tag, and an RBGpolyA signal was cut out from the pCAGGS-BDNF-HA and subcloned into the EcoRV site of pPGK-ATG-FRT (no EcoRI) vector. A loxP-STOP-loxP cassette was cloned immediately upstream of the BDNF cDNA to generate the conditional BDNF-overexpressing construct. The procedure to flip-in the conditional BDNF-overexpressing construct into the modified collagen 1a1 locus in ES cells was done as previously described (Hochedlinger et al., 2005). Hygromycin-resistant ES clones were analyzed by Southern blot. Correctly targeted ES clones were expanded and frozen. For diploid blastocyst injections, fertilized zygotes were isolated from the oviducts of day 0.5 pregnant B6D2F1 females and allowed to develop to the blastocyst stage in culture. About ten ES cells were injected per blastocyst. Injected blastocysts were transferred into day 2.5 pseudopregnant or Swiss recipient females. Chimeric mice were bred with C57B6 mice to screen for germline transmission by coat color.

BDNF ELISA

A BDNF ELISA kit (Promega) was used to measure BDNF protein expression as per the manufacturer's instructions. All solutions were from the kit or made exactly as instructed by the manufacturer.

Brains from specified ages were freshly isolated (subdivided into subregions of the brain in certain experiments) and lysed. Total protein concentration was measured by using a Dc Protein Assay kit from BIO-RAD. An acid treatment of the brain lysate was adopted to increase the amount of free BDNF. In each assay, duplicate wells were assigned for each sample. A VERSAmax microplate reader was used to measure signal intensity from the wells. A standard curve was generated from the BDNF standard wells on each plate, using the SPF3.1.2 software. The total amount of BDNF per well was calculated based on the standard curve. The relative BDNF value was then calculated by normalizing the amount of BDNF against the total protein input.

Brain Weight, Immunohistochemistry, and CA2 Neuron Measurement

For brain weight analysis, brains were freshly isolated and weighed. For CA2 neuron measurement, brains were perfused with 4% paraformaldehyde in 0.1 M phosphate buffer (pH 7.4), postfixed in 4% paraformaldehyde overnight at 4ºC, washed in PBS, processed by a TISSUE-TEK VIP machine (Miles Scientific), and imbedded in paraffin. Five-micron serial coronal sections were taken through the whole brain. Digital pictures were taken for the CA2 region of the hippocampus. The soma area (arbitrary unit) of projection neuron was determined by tracing the outline of the neuronal cell body cut through the level of the nucleolus, using OpenLab software. For immunohistochemistry, brains were perfused with 4% paraformaldehyde in 0.1 M phosphate buffer (pH 7.4), postfixed in 4% paraformaldehyde overnight at 4ºC, cryoprotected in 20% sucrose, imbedded in OCT, and frozen on dry ice. Fifty-micron serial coronal sections were taken through the whole brain. Floating sections were stained with a rabbit polyclonal BDNF-specific antibody (Chemicon), followed by a biotinylated goat anti-rabbit secondary antibody, and visualized with an immuno-peroxidase stain (Vector).

Quantitative PCR

Total RNA was isolated by using the Absolutely RNA^{TM} RT-PCR Miniprep kit (Stratagene). One microgram of RNA from each sample was used to generate cDNA, by using the SuperScript^{TM} First-Strand Synthesis System for RT-PCR kit (Invitrogen). Two microliter of the total RT product was used for each PCR reaction. CyberGreen dye (Molecular Probes) and HotStar Taq (Qiagen) were included in the PCR mix. Two sets of primers for *Bdnf* and one set of primers for GAPDH were used. *Bdnf* set 1: 5′-AGAGCTGTTGGATGAGGACC AG-3′ (forward), 5′-CAAAGGCACTTGACTACTGAGCA-3′ (reverse). *Bdnf* set 2: 5′-TACGAGACCAAGTGCAATCCC-3′ (forward), 5′-CGCA CGTACGACTGGGTAGTT-3′ (reverse). GAPDH set: 5′-AATGGGAAG CTTGTCATCAACG-3′ (forward), 5′-GAAGACACCAGTAGACTCCAC GACATA-3′ (reverse). Triplicate reactions were run for each sample for both BDNF and GAPDH. Reactions were run on the ABI PRISM 7000 Sequence Detection System (Applied Biosystems). Threshold cycle for each reaction was determined, using the ABI Prism 7000 SDS software (Applied Biosystems). *Bdnf* values were first normalized against the GAPDH values for each sample. Normalized wild-type values were set as 100% to calculate relative values.

Dark-Cycle Running-Wheel Activity Assay

Total dark-cycle running-wheel activities were recorded in a wheel running cage connected to a Mini-counter (Opto-Varimax-Mini-A, Columbus Instruments). For each measurement, a mouse was placed at least 3 hr before the starting time into a standard laboratory mouse cage with fresh bedding. Recording started at the time when the lights were normally turned off (19:00 Eastern Standard Time) and stopped at 8:00 the next morning, 1 hr after the lights normally came back on. Wild-type activity was set as 100% to calculate relative activity in the other genotypes.

Electrophysiology

The standard artificial cerebrospinal fluid (ACSF) contained (in mM) NaCl, 126; KCl, 3; $MgSO_4$, 2; $NaHPO_4$, 1; $NaHCO_3$, 25; $CaCl_2$, 7; H_2O, 2; and Dextrose, 14. For spontaneous firing, the ACSF was modified as follows: KCl, 3.5; $MgCl_2$, 0.5; $CaCl_2$, 1. Osmolality was adjusted to 318 ± 2 mOsm. Whole-cell pipette solution contained (in mM) KCl, 20; K-Gluconate, 100; HEPES, 10; Biocytin 0.1% (w/v); Mg-ATP, 4; Na-GTP, 0.3, and Na-Phosphocreatinine, 10. Three-hundred μm thick coronal sections containing the somatosensory cortex were cut in cold ACSF using a Leica VT1000S slicer. Slices were incubated in standard ACSF at 37ºC for 15–20 min immediately after slicing and subsequently at room temperature. Slices were pre-incubated (~45 min) and perfused in modified ACSF as previously described (Maffei et al., 2004). Somatic whole-cell recordings were obtained from visually identified layer 5 (L5) pyramidal cells as previously described (Dani et al., 2005). Glass pipette electrodes (4–6 MΩ resistance) were pulled from borosilicate capillaries (World Precision Instruments, Inc, Sarasota, FL) using a Sutter P92 Flame/Brown Puller (Sutter Instruments Co, Novato, CA). All data acquisition and analysis were performed using Igor Pro (Wavemetrics, Lake Oswego, OR) software and in-house programs. Data were acquired using a Multiclamp 700A (Axon Instruments/Molecular Devices, Union City, CA) computer-controlled amplifier at 10 KHz and low-pass filtered at 3 KHz. In all experiments, slices were fixed and stained for biocytin to confirm the identity of the recorded cells.

Supplemental Data

The Supplemental Data for this article can be found online at http://www.neuron.org/cgi/content/full/49/3/341/DC1/.

Acknowledgments

We thank Drs. Jing Zhang, Laurie Jackcon-Grusby, and Rita Balice-Gordon for critically reading the manuscipt; Jessie Dausman and Ruth Flannery for assistance with mouse work; and Dongdong Fu for help with histology and immunohistochemistry. Q.C. was supported by a postdoctoral fellowship from the Rett Syndrome Research Foundation. S.N was supported by a McKnight Foundation grant. R.J. was supported by a G.E.A.R. award from the Rett Syndrome Research Foundation and by a grant from the NCI (RO1 CA087869).

Received: November 23, 2005
Revised: December 20, 2005
Accepted: December 30, 2005
Published: February 1, 2006

References

Amir, R.E., Van den Veyver, I.B., Wan, M., Tran, C.Q., Francke, U., and Zoghbi, H.Y. (1999). Rett syndrome is caused by mutations in X-linked MECP2, encoding methyl-CpG-binding protein 2. Nat. Genet. *23*, 185–188.

Angelucci, F., Brene, S., and Mathe, A.A. (2005). BDNF in schizophrenia, depression and corresponding animal models. Mol. Psychiatry *10*, 345–352.

Beard, C., Hochedlinger, K., Plath, K., Wutz, A., and Jaenisch, R. (2005). An efficient method to generate single-copy transgenic mice by site specific integration in embryonic stem cells. Genesis, in press.

Bird, A.P., and Wolffe, A.P. (1999). Methylation-induced repression–belts, braces, and chromatin. Cell *99*, 451–454.

Bonni, A., Brunet, A., West, A.E., Datta, S.R., Takasu, M.A., and Greenberg, M.E. (1999). Cell survival promoted by the Ras-MAPK signaling pathway by transcription-dependent and -independent mechanisms. Science *286*, 1358–1362.

Canals, J.M., Pineda, J.R., Torres-Peraza, J.F., Bosch, M., Martin-Ibanez, R., Munoz, M.T., Mengod, G., Ernfors, P., and Alberch, J. (2004). Brain-derived neurotrophic factor regulates the onset and severity of motor dysfunction associated with enkephalinergic neuronal degeneration in Huntington's disease. J. Neurosci. *24*, 7727–7739.

Cepeda, C., Starling, A.J., Wu, N., Nguyen, O.K., Uzgil, B., Soda, T., Andre, V.M., Ariano, M.A., and Levine, M.S. (2004). Increased GABAergic function in mouse models of Huntington's disease: reversal by BDNF. J. Neurosci. Res. *78*, 855–867.

Chen, R.Z., Akbarian, S., Tudor, M., and Jaenisch, R. (2001). Deficiency of methyl-CpG binding protein-2 in CNS neurons results in a Rett-like phenotype in mice. Nat. Genet. *27*, 327–331.

Chen, W.G., Chang, Q., Lin, Y., Meissner, A., West, A.E., Griffith, E.C., Jaenisch, R., and Greenberg, M.E. (2003). Derepression of BDNF transcription involves calcium-dependent phosphorylation of MeCP2. Science *302*, 885–889.

Dani, V.S., Chang, Q., Maffei, A., Turrigiano, G.G., Jaenisch, R., and Nelson, S.B. (2005). Reduced cortical activity due to a shift in the balance between excitation and inhibition in a mouse model of Rett syndrome. Proc. Natl. Acad. Sci. USA *102*, 12560–12565.

Ernfors, P., Lee, K.F., and Jaenisch, R. (1994). Mice lacking brain-derived neurotrophic factor develop with sensory deficits. Nature *368*, 147–150.

Fan, G., Beard, C., Chen, R.Z., Csankovszki, G., Sun, Y., Siniaia, M., Biniszkiewicz, D., Bates, B., Lee, P.P., Kuhn, R., et al. (2001). DNA hypomethylation perturbs the function and survival of CNS neurons in postnatal animals. J. Neurosci. *21*, 788–797.

Ghosh, A., Carnahan, J., and Greenberg, M.E. (1994). Requirement for BDNF in activity-dependent survival of cortical neurons. Science *263*, 1618–1623.

Guy, J., Hendrich, B., Holmes, M., Martin, J.E., and Bird, A. (2001). A mouse Mecp2-null mutation causes neurological symptoms that mimic Rett syndrome. Nat. Genet. *27*, 322–326.

Hagberg, B. (1985). Rett's syndrome: prevalence and impact on progressive severe mental retardation in girls. Acta Paediatr. Scand. *74*, 405–408.

Hagberg, B., and Hagberg, G. (1997). Rett syndrome: epidemiology and geographical variability. Eur. Child Adolesc. Psychiatry *6* (Suppl 1), 5–7.

Harrington, D.P., and Fleming, T.R. (1982). A class of rank test procedures for censored survival data. Biometrika *69*, 553–566.

Hochedlinger, K., Yamada, Y., Beard, C., and Jaenisch, R. (2005). Ectopic expression of Oct-4 blocks progenitor-cell differentiation and causes dysplasia in epithelial tissues. Cell *121*, 465–477.

Horike, S., Cai, S., Miyano, M., Cheng, J.F., and Kohwi-Shigematsu, T. (2005). Loss of silent-chromatin looping and impaired imprinting of DLX5 in Rett syndrome. Nat. Genet. *37*, 31–40.

Jones, P.L., Veenstra, G.J., Wade, P.A., Vermaak, D., Kass, S.U., Landsberger, N., Strouboulis, J., and Wolffe, A.P. (1998). Methylated DNA and MeCP2 recruit histone deacetylase to repress transcription. Nat. Genet. *19*, 187–191.

Kells, A.P., Fong, D.M., Dragunow, M., During, M.J., Young, D., and Connor, B. (2004). AAV-mediated gene delivery of BDNF or GDNF is neuroprotective in a model of Huntington disease. Mol. Ther. *9*, 682–688.

Lewis, J.D., Meehan, R.R., Henzel, W.J., Maurer-Fogy, I., Jeppesen, P., Klein, F., and Bird, A. (1992). Purification, sequence, and cellular localization of a novel chromosomal protein that binds to methylated DNA. Cell *69*, 905–914.

Maffei, A., Nelson, S.B., and Turrigiano, G.G. (2004). Selective reconfiguration of layer 4 visual cortical circuitry by visual deprivation. Nat. Neurosci. *7*, 1353–1359.

Matarazzo, V., Cohen, D., Palmer, A.M., Simpson, P.J., Khokhar, B., Pan, S.J., and Ronnett, G.V. (2004). The transcriptional repressor Mecp2 regulates terminal neuronal differentiation. Mol. Cell. Neurosci. *27*, 44–58.

Nan, X., Campoy, F.J., and Bird, A. (1997). MeCP2 is a transcriptional repressor with abundant binding sites in genomic chromatin. Cell *88*, 471–481.

Nuber, U.A., Kriaucionis, S., Roloff, T.C., Guy, J., Selfridge, J., Steinhoff, C., Schulz, R., Lipkowitz, B., Ropers, H.H., Holmes, M.C., and Bird, A. (2005). Up-regulation of glucocorticoid-regulated genes in a mouse model of Rett syndrome. Hum. Mol. Genet. *14*, 2247–2256.

Poo, M.M. (2001). Neurotrophins as synaptic modulators. Nat. Rev. Neurosci. *2*, 24–32.

Rios, M., Fan, G., Fekete, C., Kelly, J., Bates, B., Kuehn, R., Lechan, R.M., and Jaenisch, R. (2001). Conditional deletion of brain-derived neurotrophic factor in the postnatal brain leads to obesity and hyperactivity. Mol. Endocrinol. *15*, 1748–1757.

Schuman, E.M. (1999). Neurotrophin regulation of synaptic transmission. Curr. Opin. Neurobiol. *9*, 105–109.

Shahbazian, M., Young, J., Yuva-Paylor, L., Spencer, C., Antalffy, B., Noebels, J., Armstrong, D., Paylor, R., and Zoghbi, H. (2002). Mice with truncated MeCP2 recapitulate many Rett syndrome features and display hyperacetylation of histone H3. Neuron *35*, 243–254.

Shieh, P.B., and Ghosh, A. (1999). Molecular mechanisms underlying activity-dependent regulation of BDNF expression. J. Neurobiol. *41*, 127–134.

Tao, X., Finkbeiner, S., Arnold, D.B., Shaywitz, A.J., and Greenberg, M.E. (1998). Ca2+ influx regulates BDNF transcription by a CREB family transcription factor-dependent mechanism. Neuron *20*, 709–726.

Tudor, M., Akbarian, S., Chen, R.Z., and Jaenisch, R. (2002). Transcriptional profiling of a mouse model for Rett syndrome reveals subtle transcriptional changes in the brain. Proc. Natl. Acad. Sci. USA *99*, 15536–15541.

Van den Veyver, I.B., and Zoghbi, H.Y. (2000). Methyl-CpG-binding protein 2 mutations in Rett syndrome. Curr. Opin. Genet. Dev. *10*, 275–279.

Wan, M., Lee, S.S., Zhang, X., Houwink-Manville, I., Song, H.R., Amir, R.E., Budden, S., Naidu, S., Pereira, J.L., Lo, I.F., et al. (1999). Rett syndrome and beyond: recurrent spontaneous and familial MECP2 mutations at CpG hotspots. Am. J. Hum. Genet. *65*, 1520–1529.

Xiang, F., Buervenich, S., Nicolao, P., Bailey, M.E., Zhang, Z., and Anvret, M. (2000). Mutation screening in Rett syndrome patients. J. Med. Genet. *37*, 250–255.

Young, J.I., Hong, E.P., Castle, J.C., Crespo-Barreto, J., Bowman, A.B., Rose, M.F., Kang, D., Richman, R., Johnson, J.M., Berget, S., and Zoghbi, H.Y. (2005). Regulation of RNA splicing by the methylation-dependent transcriptional repressor methyl-CpG binding protein 2. Proc. Natl. Acad. Sci. USA. *102*, 17551–17558.